# SUBSIDENCE MONITORING IN SEVILLE (S SPAIN) USING MULTI-TEMPORAL InSAR


**Antonio M. Ruiz-Armenteros[(1,2,3)], Ana Ruiz-Constán[(4)], Francisco Lamas-Fernández[(5)], Jesús Galindo-Zaldívar[(4,6)], Joaquim J. Sousa[(7)], Carlos Sanz de Galdeano[(6)], J. Manuel Delgado[(2,8)], Antonio Pedrera-Parias[(9)], Sergio Martos-Rosillo[(9)], Antonio J. Gil[(1,2,3)], Miguel Caro-Cuenca[(10)], Ramon F. Hanssen[(11)]**

*[(1)] Departamento de Ingeniería Cartográfica, Geodésica y Fotogrametría, Universidad de Jaén, Campus Las Lagunillas s/n, 23071 Jaén, Spain, Email: amruiz@ujaen.es, ajgil@ujaen.es*
*[(2)] Grupo de Investigación Microgeodesia Jaén, Universidad de Jaén, Spain*
*[(3)] Centro de Estudios Avanzados en Ciencias de la Tierra (CEACTierra), Universidad de Jaén, Spain*
*[(4)] Departamento de Geodinámica, Universidad de Granada, 18071 Granada, Spain. Email: aconstan@ugr.es, jgalindo@ugr.es*
*[(5)] Departamento de Ingeniería Civil, Universidad de Granada, ETSICCP, Avda. Fuentenueva, s/n, 18071 Granada, Spain. Email: flamas@ugr.es*
*[(6)] Instituto Andaluz de Ciencias de la Tierra, CSIC-Universidad de Granada, 18071 Granada, Spain. Email: csanz@ugr.es*
*[(7)] Escola de Ciências e Tecnologia, Universidade de Trás-os-Montes e Alto Douro, Vila Real, and INESC TEC (formerly INESC Porto), Portugal. Email: jjsousa@utad.pt*
*[(8)] Progressive Systems Srl, Via della Ricerca Scientifica, UTV – Parco Scientifico, ed. PP3, Rome, Italy. Email: josemanuel.delgado@progressivesystems.it*
*[(9)] Instituto Geológico y Minero de España, Ríos Rosas 23, 28003 Madrid, Spain. Email: a.pedrera@igme.es, s.martos@igme.es*
*[(10)] TNO, The Netherlands. Email: miguel.carocuenca@tno.nl*
*[(11)] Department of Geoscience and Remote Sensing, Delft University of Technology, Delft, The Netherlands. Email: r.f.hanssen@tudelft.nl*



## ABSTRACT

Seville, with a metropolitan population of about 1.5 million, is the capital and largest city of Andalusia (S Spain). It is the 30$^{th}$ most populous municipality in the European Union and contains three UNESCO World Heritage Sites. The Seville harbour, located about 80 km from the Atlantic Ocean, is the only river port in Spain. The city is located on the plain of the Guadalquivir River. Using Multi-Temporal InSAR with ERS-1/2 and Envisat data a subsidence behavior is detected in the period 1992-2010. The geometry of the subsiding areas suggests that it should be conditioned by the fluvial dynamics of the Guadalquivir River and its tributaries. Facies distribution along the fluvial system (paleochannels, flood plains...), with different grain size and matrix proportion, may explain the relative subsidence between the different sectors.


## 1. INTRODUCTION

The landscape evolution is widely conditioned by the interaction between human activity and the natural system dynamics ([1], [2]). In addition, the natural characteristics of a determined emplacement highly determine the future development of a society. In particular, relationships between villages and rivers have been extensively analyzed (e.g. [3], [4], [5] and [6]). In fact, relevant human settlements around the world (Paris, Cairo, Shanghai, Rome, etc.) were funded near fluvial systems in order to address human requirements of freshwater, fertile soil or communication ways. In Southern Spain, the advantageous conditions provided by the Guadalquivir River (Fig. 1) favored the foundation of Seville around the 8$^{th}$ century BP and the subsequent settlements of different civilizations ([7], [8]). Recurrent floods and the growth of the area occupied by the city greatly fomented the building of bridges, embankments, channels and flood protections at the river. These hydraulic actions conditioned the channel distribution (Fig. 2) and dynamics ([9], [10]) together with other factors like climate, tectonic activity, sea level, etc. Under-consolidated fluvial sediments are highly sensitive to compaction and condition the location of subsiding sectors in urban areas. This work aims to evaluate the influence of the distribution of under-consolidated fluvial sediments on the differential subsidence affecting Seville (Southern Spain).

## 2. DATA AND METHOD

### 2.1. SAR dataset

For our study we used 54 ERS-1/2 C-band images and 19 Envisat ASAR C-band images. The ERS images were acquired between June 1992 and July 2000, along descending orbits, with an incidence angle of 23º and a 5×25 m nominal spatial resolution. The ASAR images


*Proc. 'Living Planet Symposium 2016', Prague, Czech Republic, 9–13 May 2016 (ESA SP-740, August 2016)*

were acquired between February 2003 and September 2010, along descending orbits as well, with an incidence angle of 23º at the central middle swath IS2, and a 5×25 m nominal pixel dimension. Fig. 1 shows the location of these tracks over the study area.

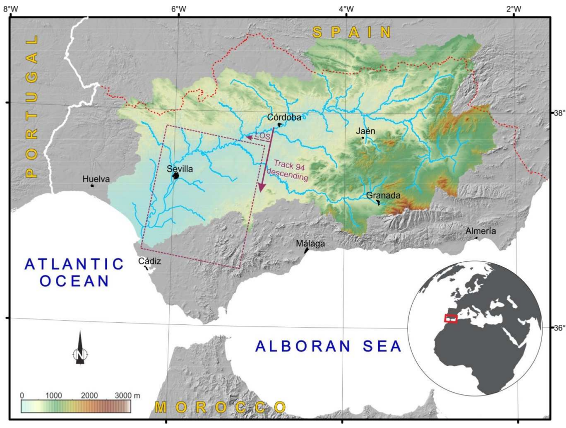


*Figure 1. Location of the study area.*

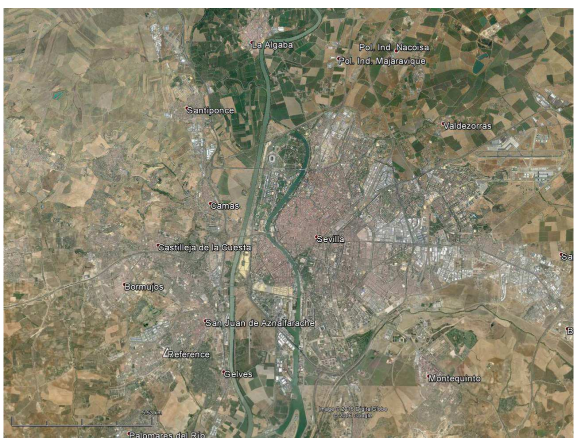


*Figure 2. Seville area over Google Earth.*

Due to ERS-2 on-board gyroscope failure, on January 2001, only images until the end of 2000 were selected to avoid high Doppler centroid differences of more than the critical value of 700 Hz. Used ERS scenes have Doppler values ranging from -487 to 318 Hz and perpendicular baselines ranging from -693,7 to 1100 m, with respect to the central reference image (master) dated August 4, 1997 (Figs. 3 and 4). ASAR scenes have perpendicular baselines ranging from -617,8 to 706,2 m with respect to the central reference image (master) dated June 2, 2008 and Doppler centroid baselines from -33 to 19 Hz (Figs. 5 and 6).

## 2.2. Multi-Temporal InSAR

Repeat pass SAR interferometry allows the Earth's surface to be scanned regularly with a given (usually fixed) revisit time.

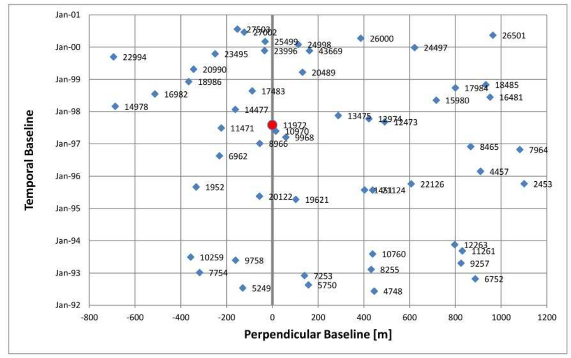


*Figure 3. Temporal vs. perpendicular baseline distribution for the ERS-1/2 dataset.*

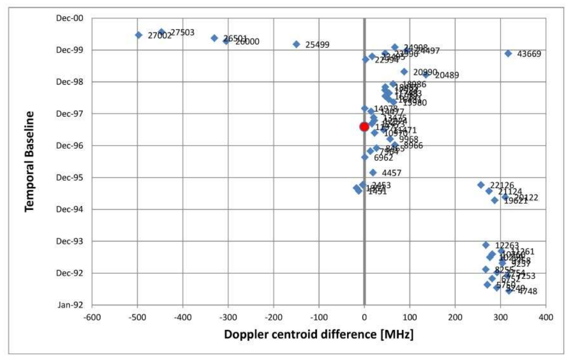


*Figure 4. Temporal vs. Dopplerr baseline distribution for the ERS-1/2 dataset.*

InSAR exploits the radar phase information of one pair of complex SAR images acquired over the same region at different times (repeat pass SAR interferometry) that are used to form an interferometric pair (the interferogram). This repeated acquisition of images over a given area is usually performed with the same sensor (or sensors) with identical system characteristics. DInSAR was described for the first time by [11], using Seasat satellite data. For a general review of SAR interferometry, the reader is referred to [12] and [13] among others.

InSAR is commonly affected by a series of limitations that should be taken into account. First of all, interferograms are affected by temporal and/or geometrical decorrelation [14]. Secondly, the interferometric phase is wrapped, and it may be quite difficult (many times impossible) to unwrap it correctly using a single interferogram [15]. Finally, even if all previous problems are solved, atmospheric artefacts may become fruitless all efforts. Multi-Temporal InSAR (MT-InSAR) techniques include solutions to some of the mentioned DInSAR limitations.

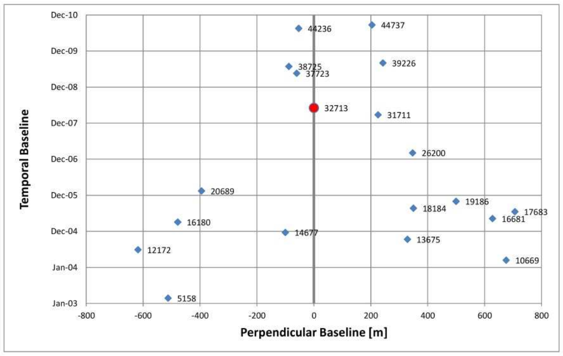


*Figure 5. Temporal vs. perpendicular baseline distribution for the Envisat dataset.*

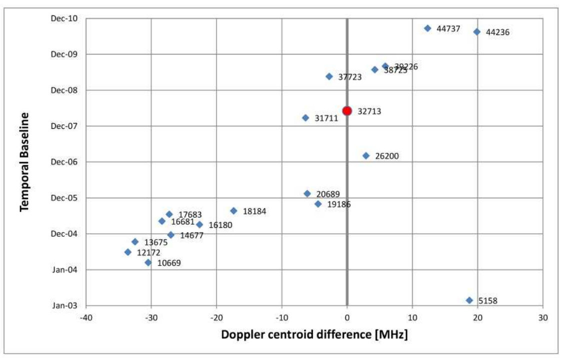


*Figure 6. Temporal vs. Dopplerr baseline distribution for the Envisat dataset.*

MT-InSAR is a group of remote sensing techniques allowing measuring and monitoring displacements of the Earth's surface over time. More generically, it can be said that MT-InSAR is a radar-based technique that belongs to the group of DInSAR. Nowadays, several MT-InSAR approaches are available, however they all exploit multiple SAR images acquired over the same area, and appropriate data processing and analysis procedures to separate phase displacement contribution from the other phase components (topography, atmosphere, etc.). This group of InSAR techniques focuses in the identification of pixels in the SAR image characterized by small phase noise which are typically related to two types of reflectors: those where the response to the radar is dominated by a strong reflecting object and remains constant over time (Persistent Scatterer, PS) and those where the response is constant over time, but is due to different small scattering objects (Distributed Scatterers, DS, or Slowly Decorrelating Filtered Phase, SDPF, pixels as they are known in StaMPS ([16], [17]), the software package used in this work.

One of the main characteristics of StaMPS is the fact that the Persistent Scatterers (PS) selection uses phase characteristics, which is suitable to find low-amplitude natural targets with phase stability that cannot be identified by amplitude-based algorithms. In other words, StaMPS uses phase spatial correlation to identify PS pixels instead of amplitude analysis as in [18], [19], [20] and [21]. An important advantage is that it does not require a prior deformation model for phase unwrapping. StaMPS evolved to an hybrid method which means that it is based on PS and DS identification, however the main outcomes of all methods remain: the deformation time series; the deformation velocity estimated over the analyzed PS/DS points and the residual topographic error, which represents the difference between the true height of the scattering phase center of a given point and the height of the DEM in this point. This is a key parameter in order to achieve an accurate geocoding.

In StaMPS, the algorithms for PS and SDFP pixels selection are basically the same. However, different interferograms are used. Single master interferograms are used for PS pixel selection, while multiple master interferograms with small baselines (SB) are used for SDFP pixels selection. Figs. 7 and 8 show the temporal vs. spatial baseline distribution for the interferometric dataset used in this study in the SB processing.

For both data stacks, ERS and ASAR we performed both PS and SB processing as well as the combination of them. For removing the phase topographic contribution we used a DEM provided by the Instituto Geográfico Nacional de España with 25 m. The inner workings of this software package are described in more detail in [16], [17], [22], [23], [24], [25] and [26].

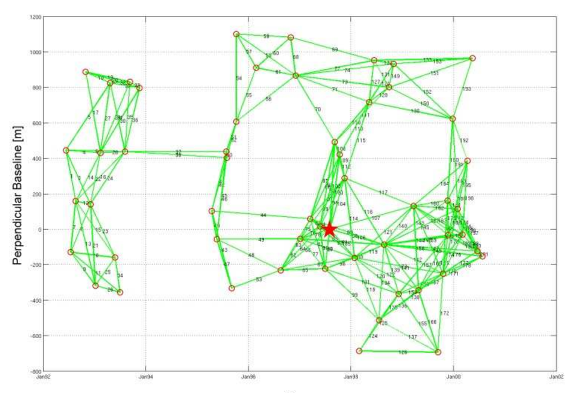


*Figure 7. Baselines distribution for SB processing of the ERS-1/2 dataset.*

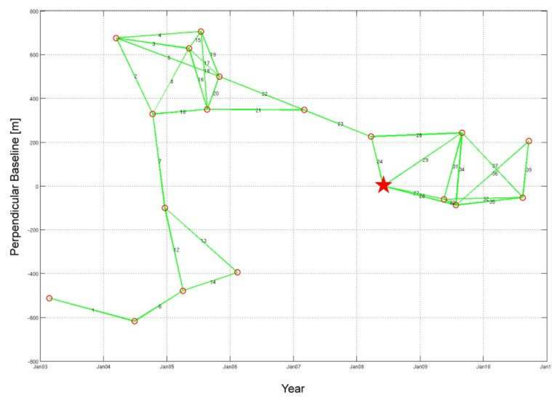


*Figure 8. Baselines distribution for SB processing of the Envisat dataset.*

## 3. RESULTS AND CONCLUSIONS

The spatial analysis of subsidence distribution shows a human-induced land deformation in Seville from 1992 to 2010 (Figs. 9 and 10).

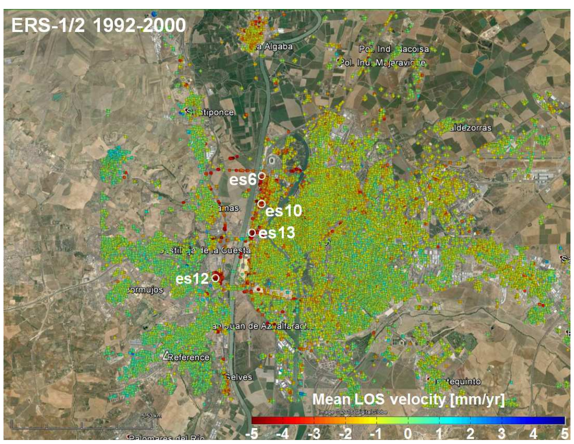


*Figure 9. Mean LOS velocity map for ERS-1/2 dataset.*

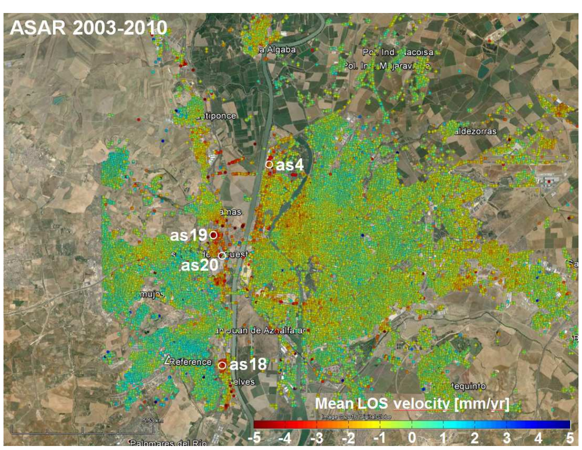


*Figure 10. Mean LOS velocity map for Envisat dataset.*

Deformation time series of points distributed along the main channel of the river show that the subsidence pattern is very similar being the most subsiding areas with LOS deformation rates in the order of -5 mm/year in both periods ERS and Envisat (Figs. 11 to 18).

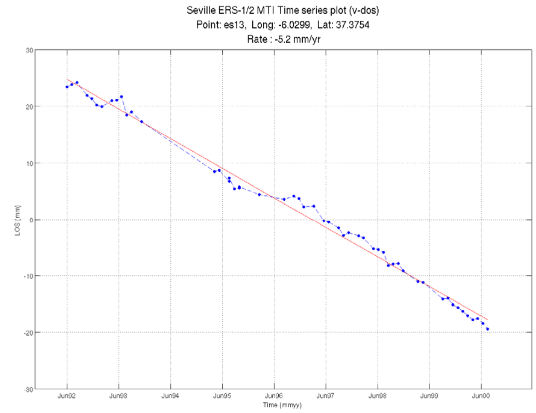


*Figure 11. Time serie of point es13 (ERS-1/2).*

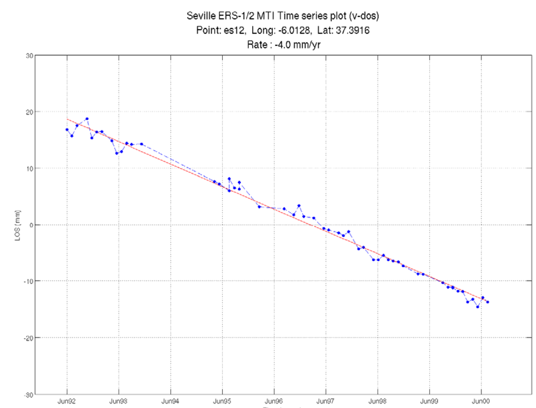


*Figure 12. Time serie of point es12 (ERS-1/2).*

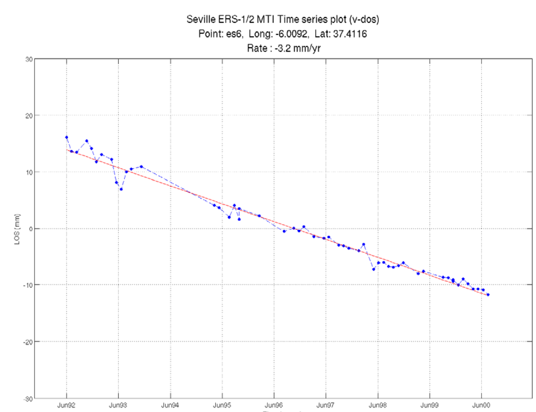


*Figure 13. Time serie of point es6 (ERS-1/2).*

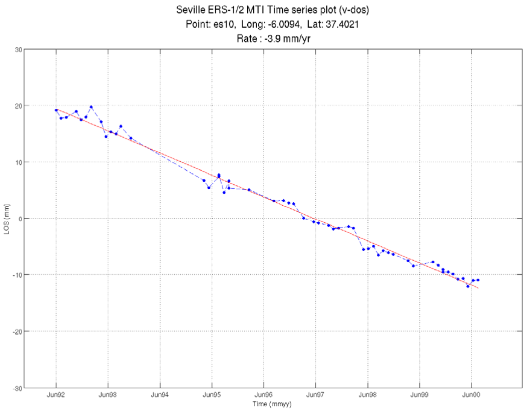


*Figure 14. Time serie of point es10 (ERS-1/2).*

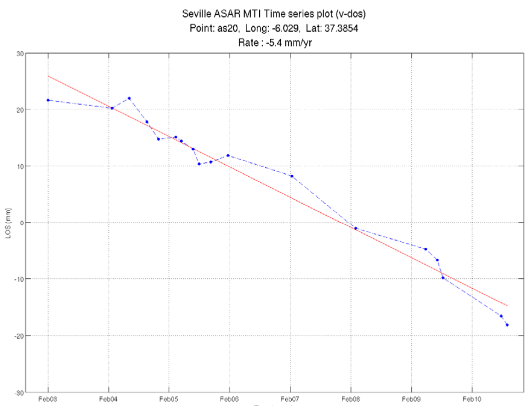


*Figure 15. Time serie of point as20 (Envisat).*

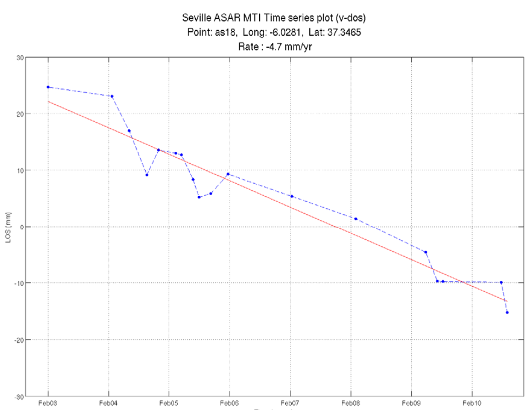


*Figure 16. Time serie of point as18 (Envisat).*

A high concentration of pixels showing medium subsidence values is preferentially located at the historical city centre, with values around -3 mm/year. On the other hand, most stables areas are restricted to the alluvial floodplain eastwards of the Guadalquivir main channel.

The main feature of this analysis is the close spatial relationship between the under-consolidated fluvial sediments distribution and subsidence. Regions where subsidence shows higher values are related to the main channel of the river and to the location of historical branches of the Guadalquivir River and its tributaries as well as abandoned meanders.

A deeper analysis of meteorological and geotechnical data available in the area could show if the tendency is related with the amount of stored water at the soil and will provide a better understanding of the detected subsidence.

Derived results could be used to implement appropriate urban planning strategies that may consider the subsidence tendency of the sectors located over under-consolidated fluvial deposits.

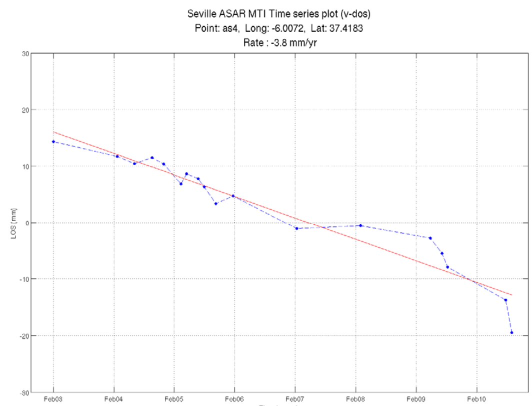


*Figure 17. Time serie of point as4 (Envisat).*

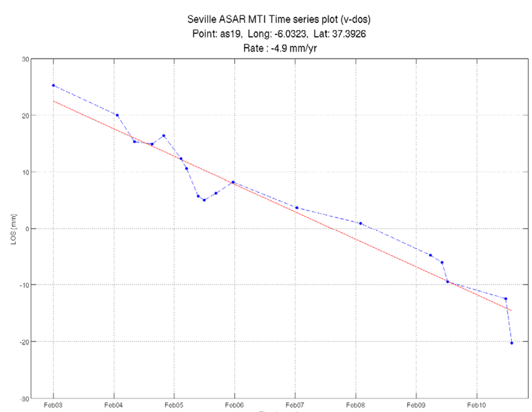


*Figure 18. Time serie of point as19 (Envisat).*

## 4. ACKNOWLEDGEMENTS

SAR data are provided by the European Space Agency (ESA) in the scope of 9386 CAT-1 project. This research was supported by PRX 12/00297 and ESP2006-28463 projects from Ministerio de Ciencia e Innovación (Spain), and UJA2015/08/05 and CEACTierra projects from University of Jaén (Spain), In addition, it was supported by the RNM-282 research group from the Junta de Andalucía (Spain). Interferometric data were processed using the public domain SAR processor DORIS and StaMPS/MTI. The DEM is freely provided by Instituto Geográfico Nacional de España. The satellite orbits used are from Delft University of Technology and ESA.

## 5. REFERENCES

1. Thomas Jr.,W.L. (Ed.) (1956). Man's Role in Changing the Face of the Earth. University Press, Chicago.

2. Braga, G. & Gervasoni, S. (1989). Evolution of the Po River: an example of the application of historic maps. In: Petts, G.E., Möller, H., Roux, A.L. (Eds.), Historical Change of Large Alluvial Rivers: Western Europe. John Wiley & Sons, Chichester, 113–126.

3. Strahler, A.N. (1956). The nature of induced erosion and aggradation. In: Thomas, W.L. (Ed.), Man's Role in Changing the Face of the Earth. University of Chicago Press, Chicago, 621–638.

4. Wolman, M.G. (1967). A cycle of sedimentation and erosion in urban river channels. Geografiska Annaler 49A, 385–395.1. Smith, J.M., Adams, B.A. & Wilson, A. (2002). The Future for Asteroid Exploration. *Planet. Space Sci.* 285(11), 123–126. doi:0000000/000000000000 *or* http://dx.doi.org/10.0000/0000

5. Gregory, K.J. (Ed.) (1977a). River Channel Changes.Wiley, Chichester. Gregory, K.J., 1995. Human activity and palaeohydrology. In: Gregory, K.J., Starkel, L., Baker, V.R. (Eds.), Global Continental Palaeohydrology. Wiley, Chichester, 151–172.

6. Bledsoe, B.P. & Watson, C.C. (2001). Effects of urbanization on channel stability. Journal of the AmericanWater Resources Association 37, 255–270.

7. Barral, M.A. & Borja, F., (2002). Aproximación a la evolución paleogeográfica histórica del sector sur del casco antiguo de Sevilla. In: Aportaciones a la geomorfología de España en el inicio del tercer milenio, 19-23. Eds: A. Pérez González, J. Vegas and M.J. Machado.

8. Borja, F. & Barral, M.A. (2005). "Evolución histórica de la Vega de Sevilla. Estudio de Geoarqueología urbana". En: Jiménez, A. (Ed.): La Catedral en la ciudad (I). Sevilla, de Astarté a San Isidoro. Págs. 5-36. Aula Hernan Ruiz. Catedral de Sevilla.

9. Vallespí, E. (1988). Paleolítico medio de aspecto postachalense en la depresión inferior del Guadalquivir. Espacio, Tiempo y Forma, I, Preh. I, Madrid, 85-91.

10. Pellicer, M. (1996). La emergencia de Sevilla. Spal 5, 87-100.

11. Gabriel, A.K., Goldstein, R.M. & Zebker, H.A. (1989). Mapping small elevation changes over large areas: differential radar interferometry. J. Geophys. Res. 94 (B7), 9183–9191.

12. Bamler, R. & Hartl, P. (1998). Synthetic aperture radar interferometry. Inverse Probl. 14, R1–R54

13. Rosen, P.A., Hensley, S., Joughin, I.R., Li, F.K., Madsen, S.N., Rodriguez, E. & Goldstein, R.M. (2000). Synthetic aperture radar interferometry. Proc. IEEE 88 (3), 333–382

14. Hanssen, R.F. (2001). Radar Interferometry: Data Interpretation and Error Analysis, Kluwer Academic Publishers, Dordrecht, The Netherlands.

15. Ghiglia, D.C. & Pritt M. D. (1998).Two-Dimensional Phase Unwrapping: Theory, Algorithms, and Software. ISBN: 978-0-471-24935-1. 512 pages. April 1998.

16. Hooper, A, Segall P. & Zebker H (2007). Persistent scatterer InSAR for crustal deformation analysis, with application to Volcán Alcedo, Galápagos. J Geophys Res 112:B07407. doi:10.1029/2006JB004763

17. Hooper, A (2008). A multi-temporal InSAR method incorporating both persistent scatterer and small baseline approaches. Geophys Res Lett 35:L16302. doi:10.1029/2008GL034654

18. Ferretti, A., Prati, C. & Rocca, F. (2001). Permanent scatterers in SAR interferometry. IEEE TGRS 39 (1), 8–20

19. Colesanti, C. & Wasowski, J. (2006). Investigating landslides with space-borne Synthetic Aperture Radar (SAR) interferometry. Eng. Geol. 88 (3), 173–199

20. Kampes, B.M. (2006). Radar Interferometry: Persistent Scatterer Technique. Springer, Dordrecht, The Netherlands

21. Ketelaar, V.B.H.G. (2009). Satellite Radar Interferometry, Subsidence Monitoring Techniques, edn, Vol., pp. Pages

22. Hooper AJ (2006). Persistent scatterer radar interferometry for crustal deformation studies and modelling of volcanic deformation. Ph.D. thesis, Stanford University

23. Hooper A (2010). A statistical-cost approach to unwrapping the phase of InSAR time series. European Space Agency ESA SP-677 (Special publication)

24. Hooper A, Zebker H, Segall P, & Kampes B (2004). A new method for measuring deformation on volcanoes and other natural terrains using InSAR persistent scatterers. Geophys Res Lett 31:L23611.doi:10.1029/2004GL021737

25. Sousa J, Hooper A, Hanssen R, Bastos L & Ruiz A (2011). Persistent scatterer InSAR: a comparison of methodologies based on a model of temporal deformation vs. spatial correlation selection criteria. Remote Sens Environ 115(10):2652–2663

26. Sousa J, Ruiz A, Hanssen R, Bastos L, Gil A, Galindo-Zaldívar J & Sanz de Galdeano C. (2010). PS-InSAR processing methodologies in the detection of field surface deformation—study of theGranada Basin (Central Betic Cordilleras, Southern Spain). J Geodyn 49:181–189. doi:10.1016/j.jog.2009.12.002